DOI: https://doi.org/10.26896/1028-6861-2023-89-9-48-52

INFLUENCE OF THE IRON ADDITIVE ON THE MICROSTRUCTURAL BEHAVIOR OF AN ALUMINUM-COPPER FOUNDRY ALLOY B206

© **Rassim Younes,[1]* Mohamed Bournane,[2] Abdelhek Idir,[1] Issam Bouklouche,[1] Mohand Amokrane Bradai,[1] Abdelhamid Sadeddine[1]**

[1] Laboratoire de Mécanique, Matériaux et énergétique (L2ME), Faculté de Technologie, Université de Bejaia, 06000 Bejaia, Algérie; e-mail: rassim.younes@univ-bejaia.dz
[2] Université du Québec à Chicoutimi, 255 Boulevard de Université, Chicoutimi, QC G7H 2B1, Canada.

Received January 12, 2023. Revised March 14, 2023. Accepted April 17, 2023.

Although used and studied since the beginning of the century, the mechanical properties of aluminum-based structural hardening alloys still conceal some secrets that metallurgists are trying to uncover. In this work we are interested in aluminum alloys and more particularly in an Al-Cu alloy. The main objective of this work was to study the influence of structural hardening heat treatments on the evolution of the mechanical and structural properties of B206 alloys. For that, we used several experimental methods adapted to this kind of scientific work. We quote essentially: the thermal treatments of setting in hardening, as well as measurements of the hardness. The analysis of the experimental results obtained by these methods allowed us to explain and to affirm that Al-Cu alloys do not give appreciable structural hardening; because of the difficulty of diffusion of iron and silicon which influences the treatment and brought in a general way to the precipitation of the phase β; plays an important role in the evolution of the mechanical characteristics of Al-Cu alloys.

Keywords: aluminum; Vickers hardness; microstructure.

INTRODUCTION

Aluminum in its pure state has poor mechanical characteristics making it impossible to use in the construction of mechanical structures. On the other hand, the addition of additive elements with adequate heat treatments causes the precipitation of a number of phases in the aluminum matrix. It should be noted that there are several families of wrought aluminum alloys that differ in their main additive elements; Al-Cu (2000 series), Al-Mn (3000 series), Al-Si (4000 series), Al-Mg (5000 series), Al-Mg-Si (6000 series) and Al-Mg-Zn alloys (7000 series). The low density of aluminum alloys with good mechanical strength is of interest to the transportation industry (rail, ship, road, aerospace) [1 – 4]. Currently, aluminum alloys are widely used to reduce the weight of the vehicle and therefore save energy [5 – 7].

Aluminium-copper foundry alloy B206 is a widely used material in the automotive and aerospace industries due to its excellent combination of mechanical properties and casting characteristics. The B206 alloy had generally dendritic microstructure with intermetallic compounds distributed along the grain boundaries [8, 9]. The previous research show clearly the presence of copper-rich particles, identified as $CuAl_2$ and CuAl phases, which has a significant effect on the mechanical properties of the alloy [10, 11].

Precipitation in aluminum alloys and the phenomenon of structural hardening are typical examples of a scientific problem where industrial innovation, research work and characterization equipment are progressing over time [12 – 16]. The mechanisms of structural hardening involve the blocking of dislocations by fine objects. The precipitation of a new phase from a supersaturated solid solution is the basis for structural hardening of alloys. The hardening of aluminum alloys by precipitation is characterized by the qualitative knowledge of the precipitation sequence and its influence on their mechanical properties [17 – 20].

The objective of this work is to study the influence of the addition of the element Iron on the microstructural behavior of the foundry alloy Al-Cu B206 in the cast state and in the naturally aged state. The work we have done, had as main objective, to study the influence of structural hardening heat treatments on the evolution of mechanical and structural properties of the alloy B206. For that, we used several experimental methods adapted to this kind of scientific work. We quote essentially: the thermal treatments of setting in hardening as well as measurements of hardness. In this study, the effect of heat treatment linked to microstructure and mechanical properties of B206 alloy were investigated using optical microscopy, X-ray diffraction (XRD), and mechanical testing.

EXPERIMENTAL PROCEDURES

Materials. In this study, a commercial aluminum-copper alloy type B206 provided by the Center

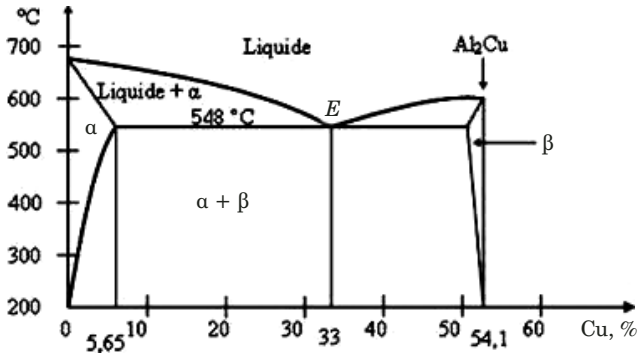

Fig. 1. Al-Cu equilibrium diagram

for Aluminum Research University of Quebec at Chicoutimi (Canada) was used, and its chemical composition is given in Tables 1 and 2. The alloy of the material was coded as follows: A(1106) and was developed from B206 base alloy with a Fe/Si = 1.83 ratio (Fig. 1). The material alloy has a low titanium content which is about 0.02 %. Their microstructures present large grains (≥70 μm) which thus favor an increased tendency to hot cracking which is a major defect for this family of alloys. Recent studies have shown that the Fe/Si ratio tends to reduce this major defect [21, 22].

Samples preparation. The specimens were fabricated from B206 bars in the cast state with a diameter of 12 mm and a thickness of 8 mm (Fig. 2). The specimens were subjected to different heat treatments.

Sample A0 was heat treated at temperature of 480°C for 2 h, followed by a rapid increase to 520°C within 1 hour. Subsequently, the specimens were maintained at 500°C for 2 h, after which the temperature was increased to 527°C in 1 h, and the specimens were kept at 527°C for 8 h. Finally, the specimens were quenched in water.

A21: Immediately after quenching, some samples undergo natural aging for 21 days.

A42: Immediately after quenching, other samples undergo natural aging for 42 days.

Method of characterization. The microstructure observations of the samples were carried out by metallographic observation using an LEICA DM LM optical microscope, equipped with a CCD camera coupled to a microcomputer. The X-ray diffraction analysis were recorded using an X'PERT PRO MRD type diffractometer from PANalytical, equipped with a copper anode X-ray tube. An acquisition time of 40 sec per angular step of 0.04° was used over the interval ranging from 40 to 100° (2θ). The identification of the crystalline phases were made by comparing the observed lines with those of the appropriate phases contained in the database.

The microhardness measurements are made on polished surfaces using a Vickers microhardness

Fig. 2. The samples based on B206 alloy

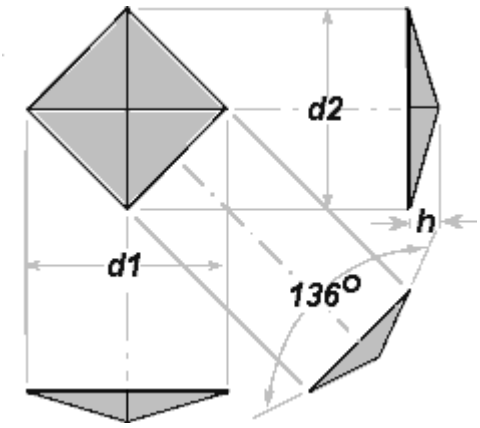

Fig. 3. Representative image of the Vickers hardness indenter

tester frome Zeiss instrument (Fig. 3). Measurements were performed on the polished surface using 200 g load and three tests were performed for each sample.

RESULTS AND DISCUSSIONS

Microstructures caracterization. There was no obviously agglomerated structure on the flat surface, and no obvious cracks, faults and other defects, only a few small pores were found. It can be see frome Fig. 4 that the microstructure had two phases (a white phase and a black phase). We also notice the appearance of black precipitates in the form of lamellae on the grain boundaries and greyish spots on the matrix, probably inclusions. Therefore, some difrence in morphologies of theses samples can be highlighted, is that for the sample A0 obtained in the cast state (Fig. 4, *a*), the grain boundaries are wide and coarse but with the aging time of 21 days for the sample A2 (Fig. 4, *b*), the

Table 1. Chemical composition of B206 alloy, wt. %

Elements	Al	Cu	Si	Fe	Mn	Mg	Ni
Composition	bal	4.60	0.01	0.06	0.40	0.25	<0.01

Table 2. Chemical compositions of B206 alloys with iron and silicon additions, wt. %

Elements	Al	Cu	Si	Fe	Mn	Mg	Ni
Composition	bal	4.59	0.06	0.11	0.23	0.25	<0.01

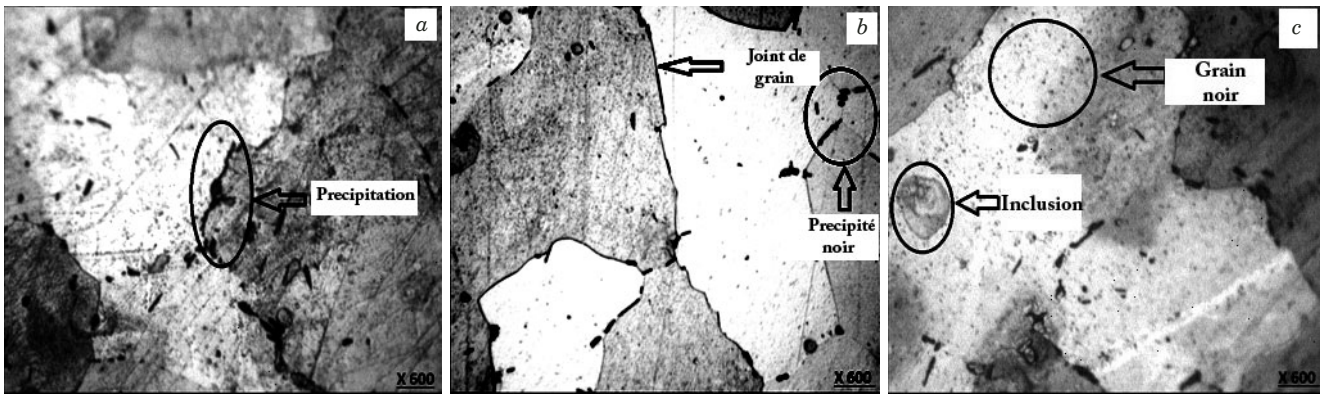

Fig. 4. Microstructure of aluminum alloy samples A0 (*a*), A21 (*b*), A42 (*c*)

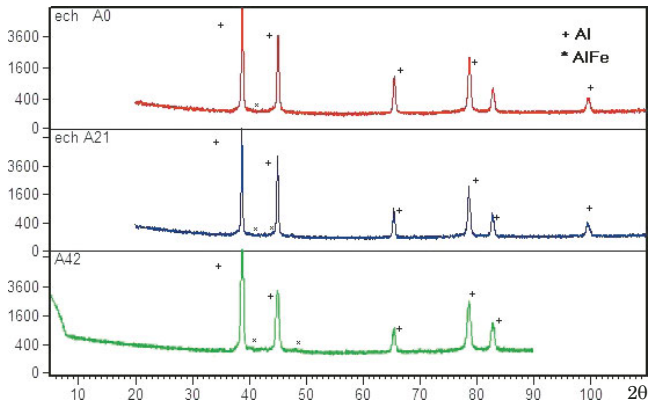

Fig. 5. X-ray diffraction spectrum of aluminum-based alloy samples A0, A21, A42

boundaries start to become finer and narrower. In contrast, sample A42 (Fig. 4, *c*) aged at 42 days shows small black grains at the grain boundaries. This can be explained by the segregation of iron.

Structural analysis by X-ray diffraction. Fig. 5 shows the XRD patterns of the samples. It can be clearly observed that the alloy phases clearly show very weak peaks associated with the very minority Al-Fe and Al_7Cu_2Fe phases; these phases are probably also present in samples A0, A21 and A42 but in even lower proportions, which makes their peaks barely perceptible. This is related to the higher percentage of Iron. While the rest of the elements (including Si) are assimilated in the Aluminum (Al) matrix; the values of the crystalline parameter a of this solution are slightly larger since only Si, among the elements present, has a larger atomic volume than Aluminum and the proportions of the other elements are practically unchanged.

Table 3. FWHM widths of the different peaks of the treated Aluminum B206

Samples	A0	A21	A42
FWHM(111)	0.2711	0.1434	0.4123
FWHM(200)	0.281	0.1764	0.469

We also calculated the FWHM widths of the different peaks at the midpoint of the Al that reflect the residual stresses. The results are presented in Table 3.

The FWHM widths mesearement reported in Table 3 demonstrate that the width of the peaks is more reduced in this order 21 days, raw and then at 42 days for the 2 types of samples. For the same class of sample A we can deduce that the stresses are more reduced in the samples at 21 days, considering that the contributions of the device and the sizes of crystallites are invariable since the recording was made by the same device and the samples underwent aging only at room temperature.

Vickers microhardness measurement. The microhardness of samples after heat treatment are determined and the same is compared with the values found from the two phases (Fig. 6). It can be seen that or the samples of the alloy family A, the black grains represented by the black phase are harder than the white grains represented by the white phase. In contrast, the dark phases of the samples A0 and A42 shows a higher microhardnesses than the samples having undergone an aging of 21 days A21 whereas the same observation is noticed for the white phases. This is probably due to the segregation of elements that can contribute to the hardening or softening of the material.

It is believed that the hardening mechanisms in crystalline materials are varied and therefore result from a decrease in the mobility of dislocations. In fact, the hardening a metal makes it potentially more fragile. It is then a question of finding a compromise between a greater resistance and an ability to deform. One of the causes of hardening can be attributed to interactions between dislocations. Indeed, when the deformation starts, the numerous dislocations created will interact to form an entanglement. The dislocations eventually become immobilized and the movement of new dislocations is considerably slowed down as they pass through this “forest” of immobile dislocations [23 – 26]. Heat treatments consist of maintaining at a high

enough temperature to dissolve the excess intermetallic phases and to level the concentrations in the solid solution [27 – 29]. As it was verified by L. Kiarodova et al., R. Carvalho et al. [30], the quenching conditions do not have, within the current limits, a great influence on the structure and properties of aluminous alloys.

CONCLUSIONS

The present work focuses on an experimental study on on the microstructure of B206 Al-Cu alloys which present problems such as: hot cracking and degradation of mechanical properties. In this attempt, the study focuses mainly on the origin of these problems caused by impurities such as Iron etc. The effect of the addition of the Iron and Silicon elements and the influence of the Iron/Silicon ratio on the microstructural behavior of the Al-Cu B206 casting alloy in the cast state and natural aging were invistigated. The main results obtained showed that:

the microstructures of the samples have two phases (white phase and black phase). They also revealed the appearance of black precipitates in the form of lamellae on the grain boundaries of all the samples;

results highlighted, that for the sample A0 obtained in the cast state, the grain boundaries are wide and coarse for the sample A0, but with the aging time of 21 days for the same sample, the boundaries start to become finer and narrower;

the X-ray diffraction analysis showed the presence of low intensity peaks associated with the parasitic phases AlFe and Al_7Cu_2Fe, which are in a very small minority on the type A samples. This is due to the low iron content;

the FWHM results showed that the residual stresses are lower for the samples aged at 21 days, but even more so for the A21 sample;

the hardness tests indicated an increase in the Vickers hardness of the samples of the A family with natural aging.

In the light of all these results, it can be concluded that natural aging at 21 days has a beneficial role on the improvement of mechanical properties for alloys. The addition of iron in large proportions to the raw alloy B206 has a negative effect on the microstructure of the alloy while silicon has no effect on the microstructure.

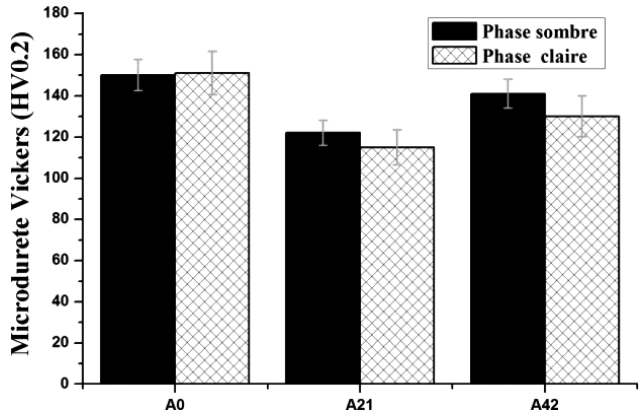

Fig. 6. Microhardness of the phases present in different microstructures under study

REFERENCES

1. **Kamal Jayaraj R., Malarvizhi S., Balasubramanian V.** Optimizing the micro-arc oxidation (MAO) parameters to attain coatings with minimum porosity and maximum hardness on the friction stir welded AA6061 aluminium alloy welds / Defence Technology. 2017. N 13. P. 111 – 117. DOI: 10.1016/j.dt.2017.03.003
2. **Wang Xf., Guo Mx., Cao Ly., et al.** Effect of rolling geometry on the mechanical properties, microstructure and recrystallization texture of Al-Mg-Si alloys / Int. J. Miner Metall Mater. 2015. N 22. P. 738 – 747. DOI: 10.1007/s12613-015-1129-4
3. **Kolbeinsen L.** The beginning and the end of the aluminium value chain Matériaux & Techniques / Norwegian University of Science and Technology — NTNU. 2020. Vol. 108. P. 506.
4. **Ganjehfard K., Taghiabadi R., Noghani M., et al.** Tensile properties and hot tearing susceptibility of cast Al-Cu alloys containing excess Fe and Si / Int. J. Miner. Met. Mater. 2021. N 28. P. 718 – 728. DOI: 10.1007/s12613-020-2039-7
5. **Sheykh-jaberi F., Cockcroft S., Maijer D., Phillion A.** Comparison of the semi-solid constitutive behaviour of A356 and B206 aluminum foundry alloys / J. Mater. Proc. Technol. 2019. Vol. 266. P. 37. DOI: 10.1016/j.jmatprotec.2018.10.029
6. **Prach O., Trudonoshyn O., Randelzhofer P., et al.** Effect of Zr, Cr and Sc on the Al-Mg-Si-Mn high-pressure die casting alloys / Mater. Sci. Eng. A. 2019. Vol. 759. P. 603. DOI: 10.1016/j.msea.2019.05.038
7. **Bai S., Perevoshchikova N., Sha Y., Wu X.** The effects of selective laser melting process parameters on relative density of the AlSi10Mg parts and suitable procedures of the Archimedes method / Appl. Sci. 2019. Vol. 9. N 3. P. 583. DOI: 10.3390/app9030583
8. **Bai Q., Li H., Du Q., et al.** Mechanical properties and constitutive behaviors of as-cast 7050 aluminum alloy from room temperature to above the solidus temperature / Int. J. Miner. Met. Mater. 2016. Vol. 23. P. 949 – 958. DOI: 10.1007/s12613-016-1311-3
9. **D'Elia F., Ravindran C., Sediako D., et al.** Hot tearing mechanisms of B206 aluminum-copper alloy / Mater. Des. 2014. Vol. 64. P. 44. DOI: 10.1016/j.matdes.2014.07.024
10. **Yakovleva A. O., Belov N. A., Bazlova T. A.,** et al. Effect of Low-Melting Metals (Pb, Bi, Cd, In) on the Structure, Phase Composition, and Properties of Casting Al – 5% Si – 4% Cu Alloy / Phys. Met. Metallogr. 2018. Vol. 119. P. 35 – 43. DOI: 10.1134/S0031918X18010167
11. **Belov N. A., Stolyarova O. O., Yakovleva A. O.** Effect of lead on the structure and phase composition of an Al – 5% Si – 4% Cu casting alliy / Russ. Met. (Metally). 2016. P. 198 – 206.
12. **Ranganatha R., Kumar V., Anil Nandi S., et al.** Multi-stage heat treatment of aluminum alloy AA7049 / Trans. Nonferr. Met. Soc. China. 2013. Vol. 23. DOI: 10.1016/S1003-6326(13)62632-1
13. **Spigarelli S., Evangelista E., McQueen H.** Study of hot workability of a heat treated AA6082 aluminum alloy / Scripta Mater. 2003. N 49. P. 179 – 183. DOI: 10.1016/S1359-6462(03)00206-9
14. **Zakir Hussain U. Khan, Chanda A., Ritura Jangid.** Fabrication and Hardness Analysis of F-MWCNTs Reinforced Aluminium Nanocomposite / Proc. Eng. 2017. Vol. 173. P. 1611 – 1618. DOI: 10.1016/j.proeng.2016.12.262

15. **Pérez-Bustamante R., Bolaños-Morales D., Bonilla-Martínez J., et al.** Microstructural and hardness behavior of graphene-nanoplatelets/aluminum composites synthesized by mechanical alloying / J. Alloys Compounds. 2014. Vol. 615. P. 578 – 582. DOI: 10.1016/j.jallcom.2014.01.225
16. **Lei Deng, Xinyun Wang, Junsong Jin, et al.** Spring back and hardness of aluminum alloy sheet part manufactured by warm forming process using non-isothermal dies / Proc. Eng. 2017. Vol. 207. P. 2388 – 2393. DOI: 10.1016/j.proeng.2017.10.1013
17. **Tiryakioğlu M., Robinson J., Salazar-Guapuriche M., et al.** Hardness-strength relationships in the aluminum alloy 7010 / Mater. Sci. Eng. A. 2015. Vol. 631. P. 196 – 200. DOI: 10.1016/j.msea.2015.02.049
18. **Surya K., Rao S., Viswanath Allamraju K.** Effect on Micro-Hardness and Residual Stress in CNC Turning of Aluminium 7075 Alloy / Mater. Today Proc. 2017. Vol. 4. Part A. P. 975 – 981. DOI: 10.1016/j.matpr.2017.01.109
19. **Sumesh Narayan, Ananthana Rayanan, Rajeshkannan.** Hardness, tensile and impact behaviour of hot forged aluminium metal matrix composites / J. Mater. Res. Technol. 2017. N 6. P. 213 – 219. DOI: 10.1016/j.jmrt.2016.09.006
20. **Kawasaki M., Saleh Alhajeri N., Cheng Xu, et al.** The development of hardness homogeneity in pure aluminum and aluminum alloy disks processed by high-pressure torsion / Mater. Sci. Eng. A. 529.2011. P. 345 – 351. DOI: 10.1007/s10853-006-0899-5
21. **Samuel A. M., Alkahtani S. A., Doty H. W., Samuel F. H.** Role of Zr and Sc addition in controlling the microstructure and tensile properties of aluminum, copper based alloys / Mater. Design. 2015. Vol. 88. P. 1134 – 1144. DOI: 10.1016/j.matdes.2015.09.090
22. **Emad M. E., Nada H. A., Besisa A. A.** Aluminum titanate based ceramics from aluminum sludge waste / Ceram. Int. 2017. Vol. 43. Issue 13. P. 10277 – 10287.
23. **Hong Hue D., Tran V., Nguyen V., et al.** High strain-rate effect on microstructure evolution and plasticity of aluminum 5052 alloy nano-multilayer: A molecular dynamics study / Vacuum. 2022. Vol. 201. P. 111104. DOI: 10.1016/j.vacuum.2022.111104
24. **Rokhlin L. L., Bochvar N. R., Leonova N. P., Sukhanov A. V.** The Effect of Additional Alloying with Sc and Sc + Zr on the Strength Properties of Al-Mg2Si Alloys / Industr. Lab. Diagn. Mater. 2015. Vol. 81. N 5 [in Russian].
25. **Petrova E., Dresvyannikov A., Galiullina N., Akhmadi Daryakenari M.** Measurements of the Size of Solid Oxide Particles by laser diffraction: Case Sudy of Aluminum Oxide / Industr. Lab. Diagn. Mater. 2015. Vol. 81. N 8 [in Russian].
26. **Sbitneva S. V., Alexeev A. A., Kolobnev N. I.** Determination of the Characteristics of the Crystal Structure of the g-type Phases in Al-Mg-Si-Cu Alloys using Dark Field Image Defocusing Method / Industr. Lab. Diagn. Mater. 2016. Vol. 82. N 12 [in Russian].
27. **Lombardi A., Sediako D., Ravindran C., Barati M.** Analysis of precipitation, dissolution and incipient melting of Al_2Cu in B206 Al alloy using in-situ neutron diffraction / J. Alloys Compounds. 2019. Vol. 784. P. 1017 – 1025. DOI: 10.1016/j.jallcom.2019.01.104
28. **Biwan Xu, Winnefeld F., Bin Ma, Rentsch D., Lothenbach B.** Influence of aluminum sulfate on properties and hydration of magnesium potassium phosphate / Cement Concrete Res. 2022. Vol. 156. DOI: 10.1016/j.cemconres.2022.106788
29. **Pragathi P., Elansezhian R.** Studies on microstructural and mechanical properties of (Nano SiC + Waste Spent catalyst) reinforced aluminum matrix composites, materials today communication / Mater. Today Comm. 2022. Vol. 30. DOI: 10.1016/j.cemconres.2022.103204
30. **Carvalho A. L., Renaudin L. B., Zara A. J., Martins J. P.** Microstructure analysis of 7050 aluminum alloy processed by multistage aging treatments / J. Alloys Compounds. 2022. Vol. 907. DOI: 10.1016/j.cemconres.2022.164400